Robotica (2009) volume 27, pp. 259–268. © 2008 Cambridge University Press
doi:10.1017/S0263574708004657 Printed in the United Kingdom

Inverse dynamics of the 6-dof out-parallel manipulator by means of the principle of virtual work

Yongjie Zhao* and Feng Gao

State Key Laboratory of Mechanical System and Vibration, Shanghai Jiao Tong University, Shanghai 200240, P.R. China.

(Received in Final Form: April 17, 2008. First published online: May 23, 2008)

SUMMARY

In this paper, the inverse dynamics of the 6-dof out-parallel manipulator is formulated by means of the principle of virtual work and the concept of link Jacobian matrices. The dynamical equations of motion include the rotation inertia of motor–coupler–screw and the term caused by the external force and moment exerted at the moving platform. The approach described here leads to efficient algorithms since the constraint forces and moments of the robot system have been eliminated from the equations of motion and there is no differential equation for the whole procedure. Numerical simulation for the inverse dynamics of a 6-dof out-parallel manipulator is illustrated. The whole actuating torques and the torques caused by gravity, velocity, acceleration, moving platform, strut, carriage, and the rotation inertia of the lead screw, motor rotor and coupler have been computed.

KEYWORDS: Out-parallel manipulator; Robot dynamics; Inverse dynamics; Principle of virtual work; Link Jacobian matrices.

1. Introduction

Parallel manipulators have been successfully used in motion simulators, robotic end-effectors, and in circumstances like fast pick-and-place operation. Due to their potential advantages, such as high accuracy, rigidity, and speed, many investigations have been carried on the parallel manipulators since the concept was introduced. In order to fully make use of the inherent characteristic, such as better dynamic performance, the dynamics must be investigated even though the kinematics of the parallel manipulator had been studied extensively during the past two decades. The dynamics of a manipulator can be used in the simulation, control, and dynamic optimum design. It plays an important role in achieving better dynamic performance. The dynamics of a parallel manipulator is very complicated due to the existence of multiple closed-loop chains. There are two types of dynamics problems for parallel manipulators[1–3]: direct dynamics and inverse dynamics. The direct dynamics problem is to find the trajectory, velocity, and acceleration of the end-effector corresponding to the actuated joint torques and/or forces. In general, it is primarily applied to the simulations of a manipulator. So the efficiency of the computation is not critical. While the inverse dynamics problem is to find the actuator torques and/or forces required to generate the desired trajectory of the manipulator. It is often used for real-time feed-forward control of a manipulator. Hence, the efficiency of the computation for the inverse dynamics is of paramount importance.

Many works[1–50] can be found on the dynamics of parallel manipulators. Several approaches have been applied to the dynamics analysis of parallel manipulators. They can be classified mainly into four categories:

1. The Newton–Euler method[4–13] formulates the dynamic equations of motion by using Newtonian mechanics. In this approach, one first writes the force and moment balances for all bodies separately and then uses the kinematical relations and the constraint forces to reduce the number of equations. This method usually requires a long computation time since it needs the exact calculation of all of the internal reactions of the constraints of the system. Although the computation of the internal reactions of constraints is useful for the purpose of design, they are not employed in the control law of the manipulator. Reference [13] presented a strategy for efficient elimination of constraint reactions to reduce the inverse dynamics computations of parallel manipulators.
2. The Lagrangian method[14–20] formulates the dynamic equations of motion by using Lagrangian functions. In this approach, one considers the constraints and kinematics of the problem first. Then, the equations of motion are written, one for each degree of freedom. The bulk of the work involved in Lagrangian mechanics is to find a proper set of generalized coordinates and to express the kinematics. Once this is done, the rest is straightforward. The formulation may contain some unknown constraint forces in Lagrangian multipliers when nonindependent generalized variables are introduced. It is required to solve the kinematic constraint equations, which leads to the additional computations.
3. Kane's method[21,22] derives the dynamic equations from a geometrical interpretation of the algorithm in terms of tangent vectors to the instantaneous configuration manifold embedded in the space of nonconstrained motion for the system. It is also straightforward for the forward dynamics, which is the characteristic of this method.[22]
4. The virtual work principle[23–34] develops dynamics equations by adopting D'Alembert's principle to formulate the equilibrium equations, which means that the work

* Corresponding author. E-mail: meyjzhao@yahoo.com.cn

performed by the external impressed forces through virtual displacements compatible with the system is zero. The constraint forces and moments of the robot system have been eliminated from the formulation. This method is used mostly for the inverse dynamics of parallel manipulators.

The inverse dynamics of parallel manipulators involve almost all of the mechanics principles. Along with these mechanics principles, many mathematical methods such as screw theory,[35] Lie algebra,[36] natural orthogonal complement,[37–39] motor algebra,[40,41] group theory,[42] symbolic programming,[42,43] geometric approach,[44] parallel computational algorithms,[45] and system identification[46] have also been adopted to the dynamics of parallel manipulators. In fact, the results of actuator forces/torques computed by different methods are equivalent.[47] Theoretically, it can be concluded that there is no trouble in modeling the dynamics of parallel manipulators. Attention should be focused on the model accuracy, computation efficiency, and practical application. However, some minute drawbacks can be found in existing papers, such as the rotation inertia of motor–coupler–screw is usually omitted from the dynamic model of parallel manipulators. This rotation inertia should be included for the exact dynamic model used for the design of the control law or the estimation of servomotor parameters for the parallel manipulators.

This paper presents a systematic methodology for the inverse dynamics, in which the rotation inertia of motor–coupler–screw and the term caused by the external force and moment exerted at the moving platform are included, of the 6-dof out-parallel manipulator by means of the principle of virtual work. The approach described here leads to efficient algorithms since the constraint forces and moments of the robot system have been eliminated from the equations of motion and there is no differential equation for the whole procedure when the principle of virtual work is applied to solve the inverse dynamics problem. Numerical simulation for the inverse dynamics of the 6-dof out-parallel manipulator is illustrated. The whole actuating torques and the torques caused by gravity, velocity, acceleration, moving platform, strut, carriage, and rotation inertia of the lead screw, rotation inertia of motor rotor and coupler have been computed. The paper is organized as follows: the description of the 6-dof out-parallel manipulator and the inverse kinematics are presented in Section 2; the velocity analysis and acceleration analysis are carried out by using the concept of link Jacobian matrix presented in ref. [28]. Then, the inverse dynamics is formulated by virtue of the principle of virtual work in Section 3. Investigations on the characteristic of dynamics and conclusions are presented in Sections 4 and 5, respectively.

2. Kinematics

2.1. 6-dof seismic simulator and platform and leg displacement conventions

The schematic diagram of the 6-dof seismic simulator is shown in Fig. 1. As shown in Fig. 1, the parallel seismic simulator is a 6PSS parallel manipulator which consists of a moving platform and six carriages. In each kinematic chain, the platform and the carriage are connected via spherical ball bearing joints by a strut of fixed length. Each carriage is driven by DC motor via a linear ball screw. The lead screw of B_1, B_2, and B_3 are vertical to the ground. The lead screw of B_4, B_5, and B_6 are parallel with the ground and are orthogonal to lead screw of B_1, B_2, and B_3.

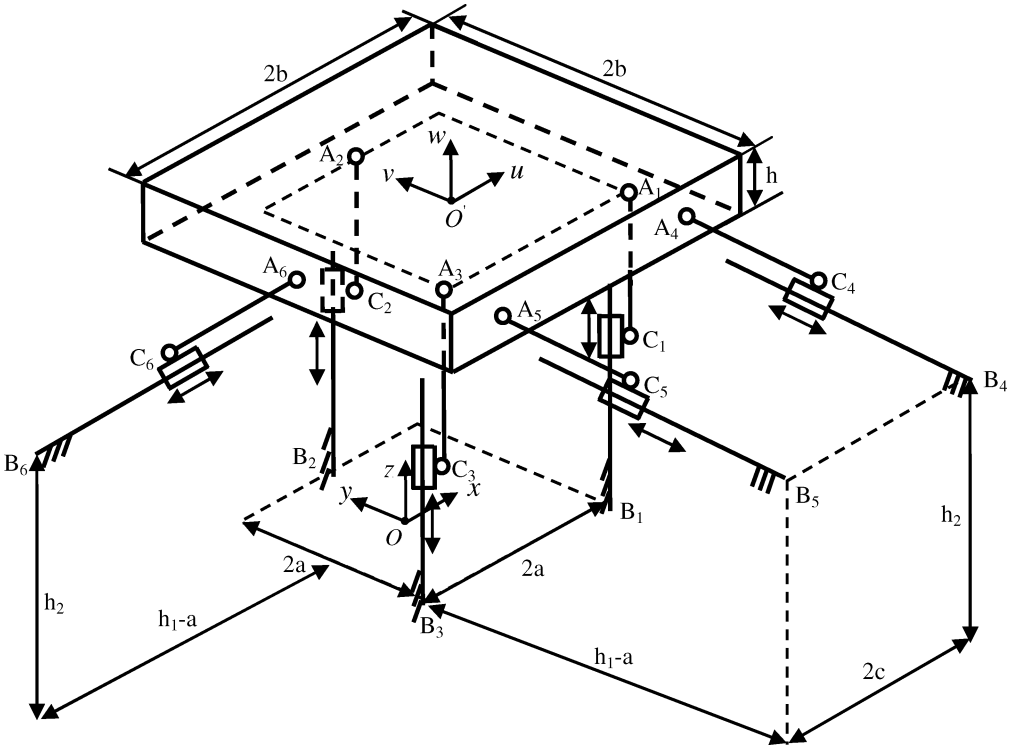

Fig. 1. Schematic diagram of the 6-dof parallel seismic simulator.

https://doi.org/10.1017/S0263574708004657 Published online by Cambridge University Press

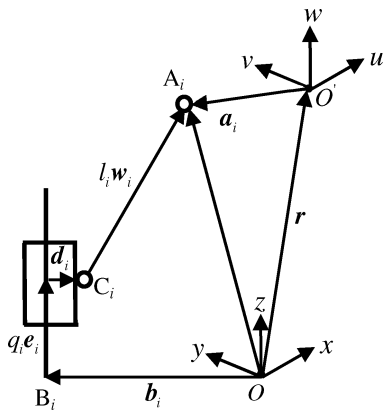

Fig. 2. Vector diagram of a PSS kinematic chain.

For the purpose of analysis, the following coordinate systems are defined. As shown in Fig. 2, the coordinate system $O-xyz$ is attached to the fixed base and another moving coordinate frame $O'-uvw$ is located at the center of mass of the moving platform. The pose of the moving platform can be described by a position vector, $\boldsymbol{r}$, and a rotation matrix, ${}^{o}\boldsymbol{R}_{o'}$. Let the rotation matrix be defined by the roll, pitch, and yaw angles, namely, a rotation of ϕ_x about the fixed x-axis, followed by a rotation of ϕ_y about the fixed y-axis, and a rotation of ϕ_z about the fixed z-axis. Thus, the rotation matrix is

$$
\begin{aligned}
{}^{o}\boldsymbol{R}_{o'} &= \mathrm{Rot}(z,\phi_z)\mathrm{Rot}(y,\phi_y)\mathrm{Rot}(x,\phi_x) \\
&= \begin{bmatrix} c\phi_z c\phi_y & c\phi_z s\phi_y s\phi_x - s\phi_z c\phi_x & c\phi_z s\phi_y c\phi_x + s\phi_z s\phi_x \\ s\phi_z c\phi_y & s\phi_z s\phi_y s\phi_x + c\phi_z c\phi_x & s\phi_z s\phi_y c\phi_x - c\phi_z s\phi_x \\ -s\phi_y & c\phi_y s\phi_x & c\phi_y c\phi_x \end{bmatrix}
\end{aligned} \tag{1}
$$

where $s\phi$ denotes the sine of angle ϕ while $c\phi$ denotes the cosine of angle ϕ. The angular velocity of the moving platform is given by

$$
\boldsymbol{\omega} = [\,\dot{\phi}_x \quad \dot{\phi}_y \quad \dot{\phi}_z\,]^T \tag{2}
$$

The orientation of each kinematic strut with respect to the fixed base can be described by two Euler angles. As shown in Fig. 3, the local coordinate system of the ith strut can be thought of as a rotation of ϕ_i about the z-axis resulting in a $C_i - x_i' y_i' z_i'$ system followed by another rotation of φ_i about the rotated y_i'-axis. So the rotation matrix of the ith strut can be written as

$$
{}^{o}\boldsymbol{R}_i = \mathrm{Rot}(z,\phi_i)\mathrm{Rot}(y_i',\varphi_i) = \begin{bmatrix} c\phi_i c\varphi_i & -s\phi_i & c\phi_i s\varphi_i \\ s\phi_i c\varphi_i & c\phi_i & s\phi_i s\varphi_i \\ -s\varphi_i & 0 & c\varphi_i \end{bmatrix} \tag{3}
$$

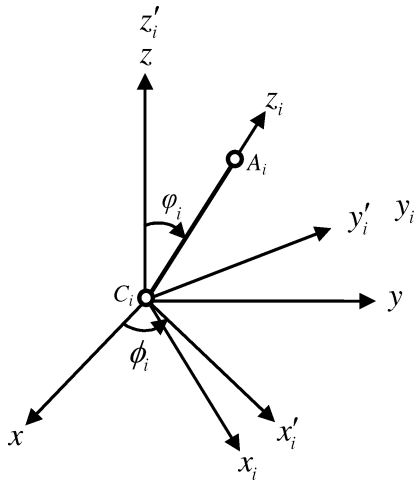

Fig. 3. The local coordinate system of the ith strut.

The unit vector along the lead screw in the coordinate system $O-xyz$ is

$$
\boldsymbol{w}_i = {}^{o}\boldsymbol{R}_i\,{}^{i}\boldsymbol{w}_i = {}^{o}\boldsymbol{R}_i \begin{bmatrix} 0 \\ 0 \\ 1 \end{bmatrix} = \begin{bmatrix} c\phi_i s\varphi_i \\ s\phi_i s\varphi_i \\ c\varphi_i \end{bmatrix} \tag{4}
$$

So the Euler angles ϕ_i and φ_i can be computed as follows:

$$
\begin{aligned}
c\varphi_i &= \boldsymbol{w}_{iz} \\
s\varphi_i &= \sqrt{\boldsymbol{w}_{ix}^2 + \boldsymbol{w}_{iy}^2}, \quad (0 \le \varphi_i < \pi) \\
s\phi_i &= \boldsymbol{w}_{iy}/s\varphi_i \\
c\phi_i &= \boldsymbol{w}_{ix}/s\varphi_i \\
\text{if } \varphi_i &= 0, \quad \text{then } \phi_i = 0.
\end{aligned} \tag{5}
$$

2.2. *Position analysis*

As shown in Fig. 2, the closed-loop position equation associated with the ith kinematic chain can be written as

$$
\boldsymbol{r} + \boldsymbol{a}_i = l_i \boldsymbol{w}_i + \boldsymbol{b}_i + \boldsymbol{d}_i + q_i \boldsymbol{e}_i \tag{6}
$$

where $\boldsymbol{r}$, q_i, $\boldsymbol{e}_i$, $\boldsymbol{w}_i$, $\boldsymbol{a}_i$, $\boldsymbol{b}_i$, and $\boldsymbol{d}_i$ denote the vector $\boldsymbol{OO'}$, the joint variable, the unit vector along the lead screw, the unit vector along strut C_iA_i, the vector $O'A_i$, the vector $\boldsymbol{OB_i}$, and the vector from the lead screw to the center point of the joint C_i, respectively.

So the inverse position solution can be achieved

$$
q_1 = A_{1z} - \sqrt{l_1^2 - (A_{1x} - a)^2 - (A_{1y} + a - d_1)^2} \tag{7a}
$$

$$
q_2 = A_{2z} - \sqrt{l_2^2 - (A_{2x})^2 - (A_{2y} - a - d_2)^2} \tag{7b}
$$

$$
q_3 = A_{3z} - \sqrt{l_3^2 - (A_{3x} + a)^2 - (A_{3y} + a - d_3)^2} \tag{7c}
$$

$$
q_4 = A_{4y} + h_1 - \sqrt{l_4^2 - (A_{4x} - c)^2 - (A_{4z} - h_2 - d_4)^2} \tag{7d}
$$

$$
q_5 = A_{5y} + h_1 - \sqrt{l_5^2 - (A_{5x} + c)^2 - (A_{5z} - h_2 - d_5)^2} \tag{7e}
$$

$$
q_6 = A_{6x} + h_1 - \sqrt{l_6^2 - (A_{6y})^2 - (A_{6z} - h_2 - d_6)^2} \tag{7f}
$$

2.3. *Velocity analysis*

Taking the derivative of Eq. (6) with respect to time yields

$$
\dot{q}_i \boldsymbol{e}_i + \boldsymbol{\omega}_i \times l_i \boldsymbol{w}_i = \boldsymbol{v} + \boldsymbol{\omega} \times \boldsymbol{a}_i \tag{8}
$$

https://doi.org/10.1017/S0263574708004657 Published online by Cambridge University Press

where $\boldsymbol{\omega}_i$ and $\boldsymbol{v}$ denote the angular velocity of the strut C_iA_i and the linear velocity of the moving platform, respectively.

Taking the dot product of both sides of Eq. (8) with $\boldsymbol{w}_i$ yields

$$\dot{q}_i = \begin{bmatrix} \dfrac{\boldsymbol{w}_i^T}{\boldsymbol{w}_i^T\boldsymbol{e}_i} & \dfrac{(\boldsymbol{a}_i \times \boldsymbol{w}_i)^T}{\boldsymbol{w}_i^T\boldsymbol{e}_i} \end{bmatrix} \begin{bmatrix} \boldsymbol{v} \\ \boldsymbol{\omega} \end{bmatrix} \tag{9}$$

Rewriting Eq. (9) in the matrix form yields

$$\dot{\boldsymbol{q}} = \boldsymbol{J}_q^{-1}\boldsymbol{J}_x\dot{\boldsymbol{X}} = \boldsymbol{J}\dot{\boldsymbol{X}} \tag{10}$$

where

$$\dot{\boldsymbol{q}} = [\,\dot{q}_1 \quad \dot{q}_2 \quad \dot{q}_3 \quad \dot{q}_4 \quad \dot{q}_5 \quad \dot{q}_6\,]^T \tag{11}$$

$$\dot{\boldsymbol{X}} = \begin{bmatrix} \boldsymbol{v} \\ \boldsymbol{\omega} \end{bmatrix} \tag{12}$$

$$\boldsymbol{J}_q = \mathrm{diag}\big(\boldsymbol{w}_1^T\boldsymbol{e}_1 \quad \boldsymbol{w}_2^T\boldsymbol{e}_2 \quad \boldsymbol{w}_3^T\boldsymbol{e}_3 \quad \boldsymbol{w}_4^T\boldsymbol{e}_4 \quad \boldsymbol{w}_5^T\boldsymbol{e}_5 \quad \boldsymbol{w}_6^T\boldsymbol{e}_6\big) \tag{13}$$

$$\boldsymbol{J}_x = \begin{bmatrix} \boldsymbol{w}_1 & \boldsymbol{w}_2 & \boldsymbol{w}_3 & \boldsymbol{w}_4 & \boldsymbol{w}_5 & \boldsymbol{w}_6 \\ \boldsymbol{a}_1 \times \boldsymbol{w}_1 & \boldsymbol{a}_2 \times \boldsymbol{w}_2 & \boldsymbol{a}_3 \times \boldsymbol{w}_3 & \boldsymbol{a}_4 \times \boldsymbol{w}_4 & \boldsymbol{a}_5 \times \boldsymbol{w}_5 & \boldsymbol{a}_6 \times \boldsymbol{w}_6 \end{bmatrix}^T \tag{14}$$

$$\boldsymbol{J} = \boldsymbol{J}_q^{-1}\boldsymbol{J}_x = [\,\boldsymbol{J}_1^T \quad \boldsymbol{J}_2^T \quad \boldsymbol{J}_3^T \quad \boldsymbol{J}_4^T \quad \boldsymbol{J}_5^T \quad \boldsymbol{J}_6^T\,]^T \tag{15}$$

where $\boldsymbol{J}$ is the *Jacobian matrix* which maps the velocity vector $\dot{\boldsymbol{X}}$ into the joint velocity vector $\dot{\boldsymbol{q}}$.

2.4. Link velocity analysis

The linear velocity of the point A_i in the $C_i - x_i'y_i'z_i'$ coordinate system is

$${}^i\boldsymbol{v}_{Ai} = \dot{q}_i\,{}^i\boldsymbol{e}_i + {}^i\boldsymbol{\omega}_i \times l_i\,{}^i\boldsymbol{w}_i = {}^i\boldsymbol{v} + {}^i\boldsymbol{\omega} \times {}^i\boldsymbol{a}. \tag{16}$$

Since ${}^i\boldsymbol{\omega}_i^{Ti}\boldsymbol{w}_i = 0$, cross-multiplying both sides of Eq. (16) with ${}^i\boldsymbol{w}_i$ allows the angular velocity of the driven parallelogram arm to be obtained as

$$\begin{aligned} {}^i\boldsymbol{\omega}_i &= \frac{1}{l_i}\big({}^i\boldsymbol{w}_i \times {}^i\boldsymbol{v}_{Ai} - {}^i\boldsymbol{w}_i \times \dot{q}_i\,{}^i\boldsymbol{e}_i\big) \\ &= \frac{1}{l_i}(S({}^i\boldsymbol{w}_i)\,{}^i\boldsymbol{v}_{Ai} - S({}^i\boldsymbol{w}_i)\dot{q}_i\,{}^i\boldsymbol{e}_i) \end{aligned} \tag{17}$$

where

$$S({}^i\boldsymbol{w}_i) = \begin{bmatrix} 0 & -{}^iw_{iz} & {}^iw_{iy} \\ {}^iw_{iz} & 0 & -{}^iw_{ix} \\ -{}^iw_{iy} & {}^iw_{ix} & 0 \end{bmatrix} \tag{18}$$

Substituting Eqs. (9) and (16) into Eq. (17) then yields

$${}^i\boldsymbol{\omega}_i = \frac{1}{l_i}\left\{\big[S({}^i\boldsymbol{w}_i)\,{}^i\boldsymbol{R}_o \quad -S({}^i\boldsymbol{w}_i)S({}^i\boldsymbol{a}_i)\,{}^i\boldsymbol{R}_o\big] - ({}^i\boldsymbol{w}_i \times {}^i\boldsymbol{e}_i) \begin{bmatrix} \dfrac{\boldsymbol{w}_i^T}{\boldsymbol{w}_i^T\boldsymbol{e}_i} & \dfrac{(\boldsymbol{a}_i \times \boldsymbol{w}_i)^T}{\boldsymbol{w}_i^T\boldsymbol{e}_i} \end{bmatrix}\right\} \begin{bmatrix} \boldsymbol{v} \\ \boldsymbol{\omega} \end{bmatrix} = \boldsymbol{J}_{i\omega} \begin{bmatrix} \boldsymbol{v} \\ \boldsymbol{\omega} \end{bmatrix} \tag{19}$$

where

$$S({}^i\boldsymbol{a}_i) = \begin{bmatrix} 0 & -{}^ia_{iz} & {}^ia_{iy} \\ {}^ia_{iz} & 0 & -{}^ia_{ix} \\ -{}^ia_{iy} & {}^ia_{ix} & 0 \end{bmatrix} \tag{20}$$

$${}^i\boldsymbol{R}_o = {}^o\boldsymbol{R}_i^{-1} = {}^o\boldsymbol{R}_i^T \tag{21}$$

The velocity of the center of the ith strut in the $C_i - x_i'y_i'z_i'$ coordinate system is

$${}^i\boldsymbol{v}_i = {}^i\boldsymbol{v}_{Ai} - {}^i\boldsymbol{\omega}_i \times \frac{l_i}{2}\,{}^i\boldsymbol{w}_i \tag{22}$$

Substituting Eqs. (9), (16), and (19) into Eq. (22) then yields

$$\begin{aligned} {}^i\boldsymbol{v}_i &= \left\{[\,{}^i\boldsymbol{R}_o \quad -S({}^i\boldsymbol{a}_i)\,{}^i\boldsymbol{R}_o\,] + \frac{l_i}{2}S({}^i\boldsymbol{w}_i)\boldsymbol{J}_{i\omega}\right\} \begin{bmatrix} \boldsymbol{v} \\ \boldsymbol{\omega} \end{bmatrix} \\ &= \boldsymbol{J}_{iv} \begin{bmatrix} \boldsymbol{v} \\ \boldsymbol{\omega} \end{bmatrix} \end{aligned} \tag{23}$$

Rewriting the linear and angular velocity of the ith strut in the matrix form yields

$$\begin{bmatrix} {}^i\boldsymbol{v}_i \\ {}^i\boldsymbol{\omega}_i \end{bmatrix} = \begin{bmatrix} \boldsymbol{J}_{iv} \\ \boldsymbol{J}_{i\omega} \end{bmatrix} \begin{bmatrix} \boldsymbol{v} \\ \boldsymbol{\omega} \end{bmatrix} = \boldsymbol{J}_{iv\omega} \begin{bmatrix} \boldsymbol{v} \\ \boldsymbol{\omega} \end{bmatrix} \tag{24}$$

where $\boldsymbol{J}_{iv\omega}$ is the *link Jacobian matrix* which maps the velocity of the moving platform in the task space into the velocity of the ith strut in the $C_i - x_i'y_i'z_i'$ coordinate system.

2.5. Acceleration analysis

Taking the derivative of Eq. (8) with respect to time gives

$$\begin{aligned} \dot{\boldsymbol{v}} = \ddot{q}_i\boldsymbol{e}_i - \dot{\boldsymbol{\omega}} \times \boldsymbol{a}_i - \boldsymbol{\omega} \times (\boldsymbol{\omega} \times \boldsymbol{a}_i) + \dot{\boldsymbol{\omega}}_i \times l_i\boldsymbol{w}_i + \boldsymbol{\omega}_i \\ \times (\boldsymbol{\omega}_i \times l_i\boldsymbol{w}_i) \end{aligned} \tag{25}$$

Taking dot product of both sides of Eq. (25) with $\boldsymbol{w}_i$ and simplifying yields

$$\begin{aligned} \ddot{q}_i &= \frac{1}{\boldsymbol{w}_i^T\boldsymbol{e}_i}\big(\boldsymbol{w}_i^T\dot{\boldsymbol{v}} + (\boldsymbol{a}_i \times \boldsymbol{w}_i)^T\dot{\boldsymbol{\omega}} + \boldsymbol{w}_i^T(\boldsymbol{\omega} \times (\boldsymbol{\omega} \times \boldsymbol{a}_i)) \\ &\quad - \boldsymbol{w}_i^T(\boldsymbol{\omega}_i \times (\boldsymbol{\omega}_i \times l_i\boldsymbol{w}_i))\big) \\ &= \boldsymbol{J}_i^T \begin{bmatrix} \dot{\boldsymbol{v}} \\ \dot{\boldsymbol{\omega}} \end{bmatrix} + \frac{1}{\boldsymbol{w}_i^T\boldsymbol{e}_i}\big((\boldsymbol{w}_i^T\boldsymbol{\omega})(\boldsymbol{a}_i^T\boldsymbol{\omega}) - (\boldsymbol{w}_i^T\boldsymbol{a}_i)(\boldsymbol{\omega}^T\boldsymbol{\omega}) \\ &\quad + l_i\,|\boldsymbol{\omega}_i \times \boldsymbol{w}_i|^2\big) \end{aligned} \tag{26}$$

https://doi.org/10.1017/S0263574708004657 Published online by Cambridge University Press

Rewriting Eq. (26) in the matrix form yields

$$\ddot{\boldsymbol{q}} = \boldsymbol{J}\ddot{\boldsymbol{X}} + \boldsymbol{V} \tag{27}$$

where

$$\boldsymbol{V} = [\, V_1 \quad V_2 \quad V_3 \quad V_4 \quad V_5 \quad V_6 \,]^T \tag{28}$$

$$V_i = \frac{1}{\boldsymbol{w}_i^T \boldsymbol{e}_i}\left(\left(\boldsymbol{w}_i^T \boldsymbol{\omega}\right)\left(\boldsymbol{a}_i^T \boldsymbol{\omega}\right) - \left(\boldsymbol{w}_i^T \boldsymbol{a}_i\right)(\boldsymbol{\omega}^T \boldsymbol{\omega}) + l_i \left|\boldsymbol{\omega}_i \times \boldsymbol{w}_i\right|^2\right) \tag{29}$$

2.6. Link acceleration analysis

Taking the derivative of Eq. (8) with respect to time in the $C_i - x_i' y_i' z_i'$ coordinate system yields

$$\begin{aligned} {}^i\dot{\boldsymbol{v}} = {} & \ddot{q}_i {}^i\boldsymbol{e}_i - {}^i\dot{\boldsymbol{\omega}} \times {}^i\boldsymbol{a}_i - {}^i\boldsymbol{\omega} \times ({}^i\boldsymbol{\omega} \times {}^i\boldsymbol{a}_i) \\ & + {}^i\dot{\boldsymbol{\omega}}_i \times l_i {}^i\boldsymbol{w}_i + {}^i\boldsymbol{\omega}_i \times ({}^i\boldsymbol{\omega}_i \times l_i {}^i\boldsymbol{w}_i) \end{aligned} \tag{30}$$

Cross-multiplying both sides of Eq. (30) with ${}^i\boldsymbol{w}_i$ yields

$$\begin{aligned} {}^i\dot{\boldsymbol{\omega}} = {} & \frac{1}{l_i}({}^i\boldsymbol{w}_i \times {}^i\dot{\boldsymbol{v}} - ({}^i\boldsymbol{w}_i \times {}^i\boldsymbol{e}_i)\ddot{q}_i - {}^i\boldsymbol{w}_i \times ({}^i\boldsymbol{a}_i \times {}^i\dot{\boldsymbol{\omega}}) + {}^i\boldsymbol{w}_i \\ & \times ({}^i\boldsymbol{\omega} \times ({}^i\boldsymbol{\omega} \times {}^i\boldsymbol{a}_i)) - {}^i\boldsymbol{w}_i \times ({}^i\boldsymbol{\omega}_i \times ({}^i\boldsymbol{\omega}_i \times {}^i\boldsymbol{w}_i))) \end{aligned} \tag{31}$$

Substituting Eq. (26) into Eq. (31) and simplifying yields

$${}^i\dot{\boldsymbol{\omega}} = \boldsymbol{J}_{i\omega}\begin{bmatrix} \dot{\boldsymbol{v}} \\ \dot{\boldsymbol{\omega}} \end{bmatrix} + \frac{1}{l_i}(\boldsymbol{\Delta}_1 + \boldsymbol{\Delta}_2) \tag{32}$$

where

$$\begin{aligned} \boldsymbol{\Delta}_1 = {} & -\frac{({}^i\boldsymbol{w}_i \times {}^i\boldsymbol{e}_i)}{\boldsymbol{w}_i^T \boldsymbol{e}_i}\left(\left(\boldsymbol{w}_i^T \boldsymbol{\omega}\right)\left(\boldsymbol{a}_i^T \boldsymbol{\omega}\right) - \left(\boldsymbol{w}_i^T \boldsymbol{a}_i\right)(\boldsymbol{\omega}^T \boldsymbol{\omega})\right. \\ & \left. + l_i \left|\boldsymbol{\omega}_i \times \boldsymbol{w}_i\right|^2\right) \end{aligned} \tag{33}$$

$$\boldsymbol{\Delta}_2 = \left({}^i\boldsymbol{\omega}_i^T {}^i\boldsymbol{a}_i\right)({}^i\boldsymbol{w}_i \times {}^i\boldsymbol{\omega}_i) - ({}^i\boldsymbol{\omega}^T {}^i\boldsymbol{\omega})({}^i\boldsymbol{w}_i \times {}^i\boldsymbol{a}_i) \tag{34}$$

Taking the derivative of Eq. (22) with respect to time yields

$$\begin{aligned} {}^i\dot{\boldsymbol{v}}_i &= {}^i\dot{\boldsymbol{v}}_{Ai} - \frac{l_i}{2} {}^i\dot{\boldsymbol{\omega}}_i \times {}^i\boldsymbol{w}_i - {}^i\boldsymbol{\omega}_i \times \left({}^i\boldsymbol{\omega}_i \times \frac{l_i}{2} {}^i\boldsymbol{w}_i\right) \\ &= {}^i\dot{\boldsymbol{v}} - S({}^i\boldsymbol{a}_i) {}^i\dot{\boldsymbol{\omega}} + S({}^i\boldsymbol{\omega}) S({}^i\boldsymbol{\omega}) {}^i\boldsymbol{a}_i + \frac{l_i}{2} S({}^i\boldsymbol{w}_i) {}^i\dot{\boldsymbol{\omega}}_i \\ &\quad - \frac{l_i}{2} S({}^i\boldsymbol{\omega}_i) S({}^i\boldsymbol{\omega}_i) {}^i\boldsymbol{w}_i \end{aligned} \tag{35}$$

Substituting Eq. (32) into Eq. (35) and simplifying yields

$$\begin{aligned} {}^i\dot{\boldsymbol{v}}_i = {} & \boldsymbol{J}_{iv}\begin{bmatrix} \dot{\boldsymbol{v}} \\ \dot{\boldsymbol{\omega}} \end{bmatrix} + S({}^i\boldsymbol{\omega}_i) S({}^i\boldsymbol{\omega}_i) {}^i\boldsymbol{a}_i + \frac{1}{2} S({}^i\boldsymbol{w}_i)(\boldsymbol{\Delta}_1 + \boldsymbol{\Delta}_2) \\ & - \frac{l_i}{2} S({}^i\boldsymbol{\omega}_i) S({}^i\boldsymbol{\omega}_i) {}^i\boldsymbol{w}_i \end{aligned} \tag{36}$$

3. Dynamics

3.1. Applied and inertia wrenches

According to the D'Alembert's principle, the force acting on the center of mass of each link consists of two parts: the inertial force and the gravity force. Similarly, the moment acting on each rigid body is the inertial moment. Assume there is no frictional force for the whole robot system. The resultant of the applied and inertia forces exerted at the center of mass of the moving platform is

$$\boldsymbol{Q}_P = \begin{bmatrix} \boldsymbol{f}_P \\ \boldsymbol{n}_P \end{bmatrix} = \begin{bmatrix} \boldsymbol{f}_e + m_p \boldsymbol{g} - m_p \dot{\boldsymbol{v}} \\ \boldsymbol{n}_e - {}^o\boldsymbol{I}_p \dot{\boldsymbol{\omega}} - \boldsymbol{\omega} \times ({}^o\boldsymbol{I}_p \boldsymbol{\omega}) \end{bmatrix} \tag{37}$$

where $\boldsymbol{f}_e$ and $\boldsymbol{n}_e$ are the external force and moment exerted at the center of mass of the moving platform, respectively, ${}^o\boldsymbol{I}_p = {}^o\boldsymbol{R}_{o'}\ {}^{o'}\boldsymbol{I}_p\ {}^{o'}\boldsymbol{R}_o$ is the inertia matrix of the moving platform taken about the center of mass expressed in the $O - xyz$ coordinate system and m_p is its mass.

Assuming that the gravitational force is the only external force, so the resultant of the applied and inertia forces exerted at the center of mass of the ith strut can be expressed in the $C_i - x_i' y_i' z_i'$ coordinate system as

$${}^i\boldsymbol{Q}_i = \begin{bmatrix} {}^i\boldsymbol{f}_i \\ {}^i\boldsymbol{n}_i \end{bmatrix} = \begin{bmatrix} m_i {}^i\boldsymbol{R}_o \boldsymbol{g} - m_i {}^i\dot{\boldsymbol{v}}_i \\ -{}^i\boldsymbol{I}_i {}^i\dot{\boldsymbol{\omega}}_i - {}^i\boldsymbol{\omega}_i \times ({}^i\boldsymbol{I}_i {}^i\boldsymbol{\omega}_i) \end{bmatrix} \tag{38}$$

where ${}^i\boldsymbol{I}_i$ is the inertia matrix of the ith cylindrical strut about their respective centers of mass expressed in the $C_i - x_i' y_i' z_i'$ coordinate system and m_i is its mass.

There is pure translational motion for the carriage, so the resultant of the applied and inertia forces exerted at the center of mass of the carriage can be expressed in the $O - xyz$ coordinate system as

$$f_{qi} = (m_{qi} \boldsymbol{g} - m_{qi} \ddot{\boldsymbol{q}}_i)^T \frac{\boldsymbol{q}_i}{\|\boldsymbol{q}_i\|} \tag{39}$$

where m_{qi} and $\ddot{\boldsymbol{q}}_i$ are the mass and the acceleration of the carriage, respectively, and $\|\boldsymbol{q}_i\|$ is the Euclidean norm of $\boldsymbol{q}_i$.

There is pure rotation motion for the lead screw, coupler, and motor rotor, so the resultant of the applied and inertia forces exerted at the screw–coupler–rotor is

$$N_i = \tau_i - (I_{\mathrm{L}i} + I_{\mathrm{C}i} + I_{\mathrm{M}i})\ddot{\theta}_i \tag{40}$$

where $I_{\mathrm{L}i}$, $I_{\mathrm{C}i}$, and $I_{\mathrm{M}i}$ are the rotary inertia of the lead screw, coupler, and motor rotor, respectively, τ_i is the input torque actuated by the motor, and $\ddot{\theta}_i$ is the angular acceleration of the screw–coupler–rotor. The relationship between the lead screw motion and the carriage motion is $\ddot{\theta}_i = \frac{2\pi}{p_i}\ddot{q}_i$, where $p_i = 0.05\ \mathrm{m}^{-1}$ is the lead of the linear ball screw. Other than the speed reduction caused by the pitch of the lead screws there is no speed reducer for the out-parallel manipulator. Otherwise the reduction ratio should be included in Eq. (40).

3.2. Equations of motion

According to the D'Alembert's principle, the principle of the virtual work can be extended from the static to the dynamic

https://doi.org/10.1017/S0263574708004657 Published online by Cambridge University Press

case. It can be stated as: The virtual work of the external forces applied to the system must be zero. For this out-parallel manipulator, it can be expressed in the formula

$$\delta \boldsymbol{x}_p^T \boldsymbol{Q}_p + \sum_{i=1}^{6} \delta^i \boldsymbol{x}_i^{Ti} \boldsymbol{Q}_i + \delta \boldsymbol{q}^T \boldsymbol{f}_q + \delta \boldsymbol{\theta}^T \boldsymbol{N} = 0 \tag{41}$$

$$\delta \boldsymbol{q} = [\,\delta q_1 \quad \delta q_2 \quad \delta q_3 \quad \delta q_4 \quad \delta q_5 \quad \delta q_6\,]^T \tag{42}$$

$$\begin{aligned} \delta \boldsymbol{\theta} &= [\,\delta\theta_1 \quad \delta\theta_2 \quad \delta\theta_3 \quad \delta\theta_4 \quad \delta\theta_5 \quad \delta\theta_6\,]^T \\ &= \operatorname{diag}\left(\frac{2\pi}{p_1} \quad \frac{2\pi}{p_2} \quad \frac{2\pi}{p_3} \quad \frac{2\pi}{p_4} \quad \frac{2\pi}{p_5} \quad \frac{2\pi}{p_6}\right) \delta \boldsymbol{q} \\ &= \boldsymbol{A}\delta \boldsymbol{q} \end{aligned} \tag{43}$$

$$\boldsymbol{f}_q = [\,f_{q1} \quad f_{q2} \quad f_{q3} \quad f_{q4} \quad f_{q5} \quad f_{q6}\,]^T \tag{44}$$

$$\boldsymbol{N} = [\,N_1 \quad N_2 \quad N_3 \quad N_4 \quad N_5 \quad N_6\,]^T \tag{45}$$

In Eq. (41), the resultant of the applied and inertia forces ${}^i\boldsymbol{Q}_i$ and its corresponding virtual displacement $\delta^i \boldsymbol{x}_i$ are expressed in the $C_i - x_i' y_i' z_i'$ coordinate system. From Eq. (24), the relationship between the above virtual displacement $\delta^i \boldsymbol{x}_i$ and the virtual displacement $\delta \boldsymbol{x}_p$ is determined by

$$\delta^i \boldsymbol{x}_i^T = \delta \boldsymbol{x}_p^T \boldsymbol{J}_{iv\omega}^T \tag{46}$$

The relationship between the virtual displacement $\delta \boldsymbol{q}$ and $\delta \boldsymbol{x}_p$ is

$$\delta \boldsymbol{q}^T = \delta \boldsymbol{x}_p^T \boldsymbol{J}^T \tag{47}$$

Substituting Eqs. (43), (46), and (47) into Eq. (41) yields

$$\delta \boldsymbol{x}_p^T \boldsymbol{Q}_p + \sum_{i=1}^{6} \delta \boldsymbol{x}_p^T \boldsymbol{J}_{iv\omega}^{T\,i} \boldsymbol{Q}_i + \delta \boldsymbol{x}_p^T \boldsymbol{J}^T \boldsymbol{f}_q + \delta \boldsymbol{x}_p^T \boldsymbol{J}^T \boldsymbol{A}^T \boldsymbol{N} = 0 \tag{48}$$

Since Eq. (48) is always valid for any $\delta \boldsymbol{x}_p$, it must follow that

$$\boldsymbol{Q}_p + \sum_{i=1}^{6} \boldsymbol{J}_{iv\omega}^{T\,i} \boldsymbol{Q}_i + \boldsymbol{J}^T \boldsymbol{f}_q + \boldsymbol{J}^T \boldsymbol{A}^T \boldsymbol{N} = 0 \tag{49}$$

So when the manipulator is not in a singular configuration, the input torque can be determined by the inverse transformation of Eq. (49)

$$\begin{aligned} \boldsymbol{\tau} &= -\boldsymbol{A}^{-T} \boldsymbol{J}^{-T} \left(\boldsymbol{Q}_p + \sum_{i=1}^{6} \boldsymbol{J}_{iv\omega}^{T\,i} \boldsymbol{Q}_i + \boldsymbol{J}^T \boldsymbol{f}_q \right) + \boldsymbol{I}_{\mathrm{LCM}} \ddot{\boldsymbol{\theta}} \\ &= -\boldsymbol{A}^{-T} \boldsymbol{J}^{-T} \left(\boldsymbol{Q}_p + \sum_{i=1}^{6} \boldsymbol{J}_{iv\omega}^{T\,i} \boldsymbol{Q}_i + \boldsymbol{J}^T \boldsymbol{f}_q \right) + \boldsymbol{I}_{\mathrm{LCM}} \boldsymbol{A} \ddot{\boldsymbol{q}} \end{aligned} \tag{50}$$

where

$$\begin{aligned} &\boldsymbol{I}_{\mathrm{LCM}} \\ &\quad = \operatorname{diag}(\, I_{\mathrm{LCM1}} \quad I_{\mathrm{LCM2}} \quad I_{\mathrm{LCM3}} \quad I_{\mathrm{LCM4}} \quad I_{\mathrm{LCM5}} \quad I_{\mathrm{LCM6}}\,) \\ &I_{\mathrm{LCM}i} = I_{\mathrm{L}i} + I_{\mathrm{C}i} + I_{\mathrm{M}i} \end{aligned} \tag{51}$$

Substituting Eqs. (37)–(40) into Eq. (50) yields

$$\begin{aligned} \boldsymbol{\tau} = &-\boldsymbol{A}^{-T} \boldsymbol{J}^{-T} \begin{bmatrix} \boldsymbol{f}_e \\ \boldsymbol{n}_e \end{bmatrix} - \boldsymbol{A}^{-T} \boldsymbol{J}^{-T} \left\{ \begin{bmatrix} m_p \boldsymbol{g} \\ \boldsymbol{0} \end{bmatrix} \right. \\ &+ \sum_{i=1}^{6} \boldsymbol{J}_{iv\omega}^T \begin{bmatrix} m_i {}^i\boldsymbol{R}_o \boldsymbol{g} \\ \boldsymbol{0} \end{bmatrix} \\ &+ \boldsymbol{J}^T \left[(m_{q1}\boldsymbol{g})^T \frac{\boldsymbol{q}_1}{\|\boldsymbol{q}_1\|} \quad (m_{q2}\boldsymbol{g})^T \frac{\boldsymbol{q}_2}{\|\boldsymbol{q}_2\|} \quad (m_{q3}\boldsymbol{g})^T \frac{\boldsymbol{q}_3}{\|\boldsymbol{q}_3\|} \right. \\ &\left. \left. \times \quad (m_{q4}\boldsymbol{g})^T \frac{\boldsymbol{q}_4}{\|\boldsymbol{q}_4\|} \quad (m_{q5}\boldsymbol{g})^T \frac{\boldsymbol{q}_5}{\|\boldsymbol{q}_5\|} \quad (m_{q6}\boldsymbol{g})^T \frac{\mathbf{q}_6}{\|\boldsymbol{q}_6\|} \right]^T \right\} \\ &+ \boldsymbol{A}^{-T} \boldsymbol{J}^{-T} \left\{ \begin{bmatrix} m_p \dot{\boldsymbol{v}} \\ {}^o\boldsymbol{I}_p \dot{\boldsymbol{\omega}} \end{bmatrix} + \sum_{i=1}^{6} \boldsymbol{J}_{iv\omega}^T \begin{bmatrix} m_i {}^i\dot{\boldsymbol{v}}_i \\ {}^i\boldsymbol{I}_i {}^i\dot{\boldsymbol{\omega}}_i \end{bmatrix} \right. \\ &\left. + \boldsymbol{J}^T [\, m_{q1}\ddot{q}_1 \;\; m_{q2}\ddot{q}_2 \;\; m_{q3}\ddot{q}_3 \;\; m_{q4}\ddot{q}_4 \;\; m_{q5}\ddot{q}_5 \;\; m_{q6}\ddot{q}_6 \;\,]^T \right\} \\ &+ \boldsymbol{I}_{\mathrm{LCM}} \boldsymbol{A} \ddot{\boldsymbol{q}} + \boldsymbol{A}^{-T} \boldsymbol{J}^{-T} \left\{ \begin{bmatrix} \boldsymbol{0} \\ \boldsymbol{\omega} \times ({}^o\boldsymbol{I}_p \boldsymbol{\omega}) \end{bmatrix} \right. \\ &\left. + \sum_{i=1}^{6} \boldsymbol{J}_{iv\omega}^T \begin{bmatrix} \boldsymbol{0} \\ {}^i\boldsymbol{\omega}_i \times ({}^i\boldsymbol{I}_i {}^i\boldsymbol{\omega}_i) \end{bmatrix} \right\} \end{aligned} \tag{52}$$

where $\boldsymbol{0} = [\,0\;0\;0\,]^T$.

From Eq. (52), it is shown that the input torques are determined by the structure parameters, the position parameters, the kinematics parameters (including the velocity and the acceleration), the gravity term and the term caused by the external force, and moment exerted at the moving platform. Substituting Eqs. (24), (31), and (36) into Eq. (52) and simplifying, the inverse dynamics model of the out-parallel manipulator is achieved

$$\boldsymbol{\tau} = \boldsymbol{D}(\boldsymbol{q})\ddot{\boldsymbol{q}} + \boldsymbol{h}(\boldsymbol{q}, \dot{\boldsymbol{q}}) + \boldsymbol{G}(\boldsymbol{q}) - \boldsymbol{A}^{-T} \boldsymbol{J}^{-T} \begin{bmatrix} \boldsymbol{f}_e \\ \boldsymbol{n}_e \end{bmatrix} \tag{53}$$

where $\boldsymbol{D}(\boldsymbol{q})$ is the inertia matrix of the manipulator, $\boldsymbol{h}(\boldsymbol{q}, \dot{\boldsymbol{q}})$ is the velocity term, and $\boldsymbol{G}(\boldsymbol{q})$ is the gravity term of the inverse dynamic equations. It can be seen that Eq. (53) changes into the static equation when the manipulator is stationary.

The constraint forces and interacting forces between particles are eliminated from the procedure when using the principle of virtual work to formulate the inverse dynamics of the parallel manipulator. The elimination of the need to consider the constraint and interacting forces is the advantage of using the principle of virtual work over the Newtonian approach.

Table I. The parameters of the base platform (m).

	1	2	3	4	5	6
x_{Bi}	0.300	0.000	−0.300	0.300	−0.300	−1.607
y_{Bi}	−0.300	0.300	−0.300	−1.607	−1.607	0.000
z_{Bi}	0.000	0.000	0.000	1.437	1.437	1.437

https://doi.org/10.1017/S0263574708004657 Published online by Cambridge University Press

Table II. The parameters of the moving platform which are measured in the coordinate frame $O' - uvw$ (m).

	1	2	3	4	5	6
x_{Ai}	0.300	0.000	−0.300	0.300	−0.300	−0.581
y_{Ai}	−0.300	0.300	−0.300	−0.581	−0.581	0.000
z_{Ai}	−0.266	−0.266	−0.266	−0.0375	−0.0375	−0.0375

Table III. The length of the strut $C_i A_i$ (m).

	1	2	3	4	5	6
l_i	0.382	0.362	0.382	0.382	0.382	0.362

Table IV. The mass parameters of the manipulator (kg).

	1	2	3	4	5	6
m_i	20	20	20	20	20	20
m_{qi}	50	100	50	50	50	100

is presented. The program based on the algorithm is developed by using the MATLAB software. The parameters of the manipulator used for the simulation are given in Tables I through IV.

The mass of the moving platform is $m_p = 200$ kg. The inertia parameters used in the simulation are given as

$$
{}^{o'}\boldsymbol{I}_p = \begin{bmatrix} 17.33 & 0 & 0 \\ 0 & 17.33 & 0 \\ 0 & 0 & 33.33 \end{bmatrix} \text{kg} \cdot \text{m}^2, \; {}^{i}\boldsymbol{I}_i
$$

$$
= \begin{bmatrix} 0.50 & 0 & 0 \\ 0 & 0.50 & 0 \\ 0 & 0 & 0.01 \end{bmatrix} \text{kg} \cdot \text{m}^2
$$

$$
I_{\text{L}i} = 10.5 \times 10^{-4} \text{ kg} \cdot \text{m}^2,
$$

$$
I_{\text{C}i} + I_{\text{M}i} = 248 \times 10^{-4} \text{ kg} \cdot \text{m}^2.
$$

4. Numerical Simulation

In this section, a numerical example for the inverse dynamics computation of the 6-dof out-parallel manipulator

Another parameter used in the simulation is given as $d_i = 0.244$ m.

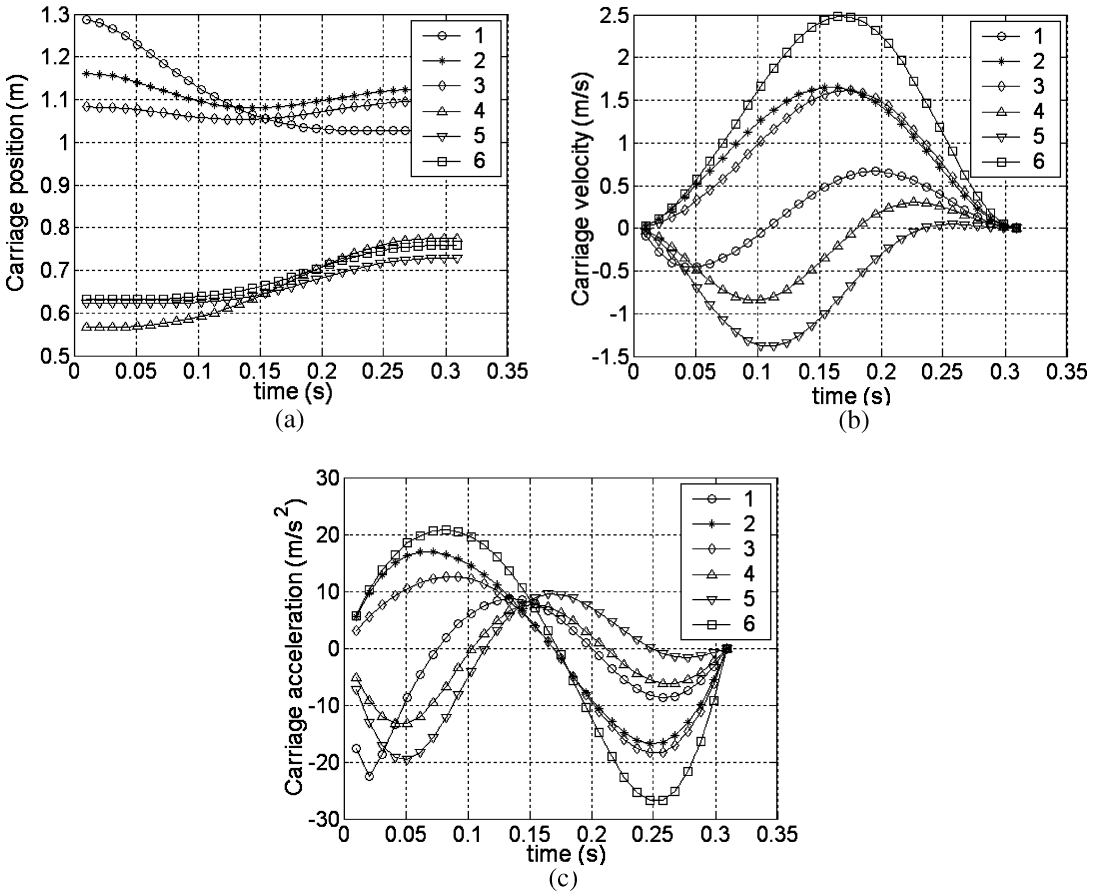

Fig. 4. Variations of carriage position (a), velocity (b), and acceleration (c) vs. time.

https://doi.org/10.1017/S0263574708004657 Published online by Cambridge University Press

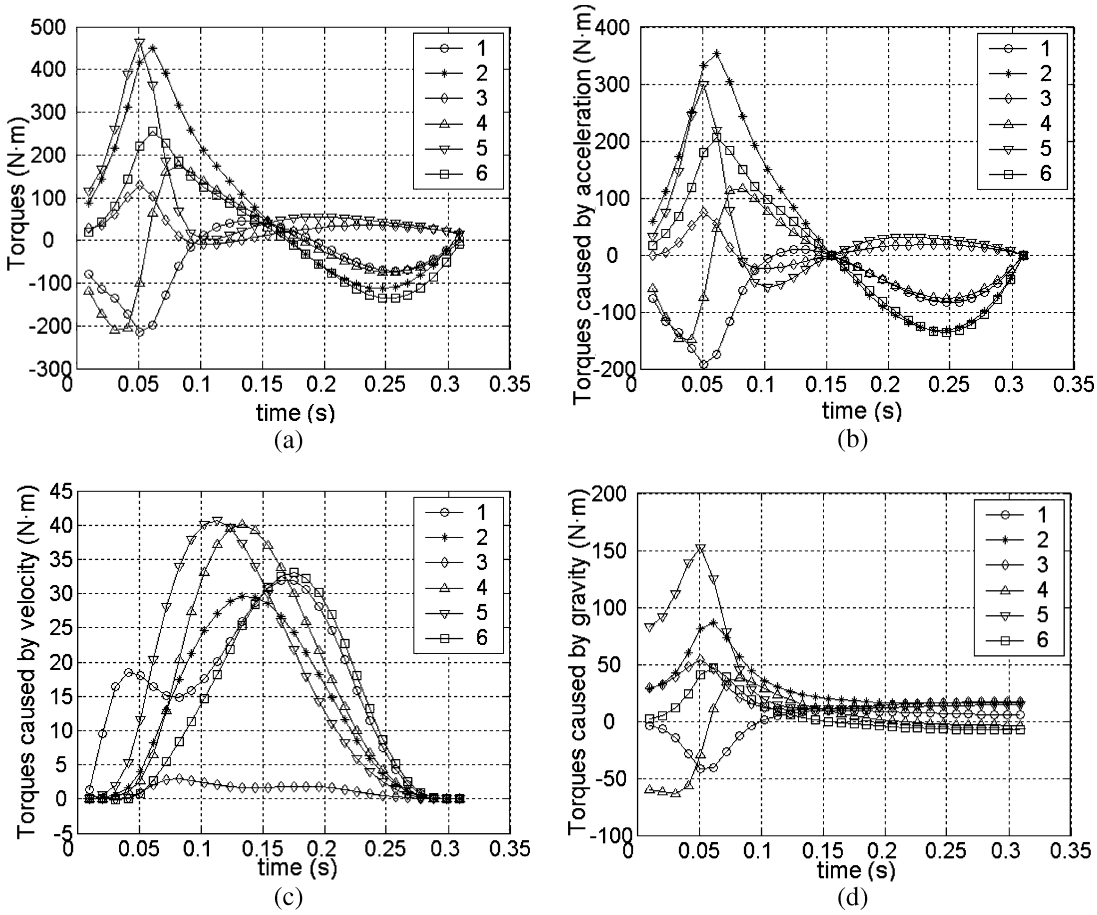

Fig. 5. Variations of whole actuating torques (a), torques caused by acceleration term (b), torques caused by the velocity term (c), and torques caused by the gravity term (d) vs. time.

The motion of the moving platform used in the numerical simulation is expressed as

$$\begin{cases} x = -0.081 + \dfrac{a_{\max} T^2}{5.7735}(10\tau^3 - 15\tau^4 + 6\tau^5) \\ y = -0.081 + \dfrac{a_{\max} T^2}{5.7735}(10\tau^3 - 15\tau^4 + 6\tau^5) \\ z = 1.6 + \dfrac{a_{\max} T^2}{5.7735}(10\tau^3 - 15\tau^4 + 6\tau^5) \\ \phi_x = -0.081 + \dfrac{a_{\max} T^2}{5.7735}(10\tau^3 - 15\tau^4 + 6\tau^5) \\ \phi_y = -0.081 + \dfrac{a_{\max} T^2}{5.7735}(10\tau^3 - 15\tau^4 + 6\tau^5) \\ \phi_z = -0.081 + \dfrac{a_{\max} T^2}{5.7735}(10\tau^3 - 15\tau^4 + 6\tau^5) \end{cases} \tag{54}$$

where $a_{\max} = 9.816\ \text{m/s}^2$, $\tau = \frac{t}{T}$, $T = \sqrt{5.7735 S / a_{\max}}$ s, and $S = 0.162$ m.

The position, velocity, and acceleration of the carriages are shown in Fig. 4.

According to Eq. (52), the whole actuating torques and the torques caused by the gravity, the velocity, and the acceleration term can be computed. The results shown in Fig. 5 imply that for this simulation the torques caused by the acceleration terms are larger than the other two terms.

According to Eq. (52), the torques caused by the moving platform, strut, carriage, and rotation inertia of the lead screw, motor rotor, and coupler are computed. They are shown in Fig. 6.

The results shown in Fig. 6 show that for this simulation, the torques caused by the rotation inertia of the motor–coupler–screw should be included for the exact dynamic model used for the design of the control law or the estimation of servomotor parameters for the parallel manipulators.

5. Conclusions

The inverse dynamics of the 6-dof out-parallel manipulator have been formulated by means of the principle of virtual work and the concept of link Jacobian matrices. The dynamical equations of motion include the rotation inertia of motor–coupler–screw and the term caused by the external force and moment exerted at the moving platform. The approach described here leads to efficient algorithms since the constraint forces and moments of the robot system have been eliminated from the equations of motion and there is no differential equation for the whole procedure. The whole actuating torques and the torques caused by gravity, velocity, acceleration, moving platform, strut, carriage, and rotation inertia of the lead screw, motor rotor, and coupler have been computed in the numerical simulation. The results shown in the simulation demonstrate that torques caused by the

https://doi.org/10.1017/S0263574708004657 Published online by Cambridge University Press

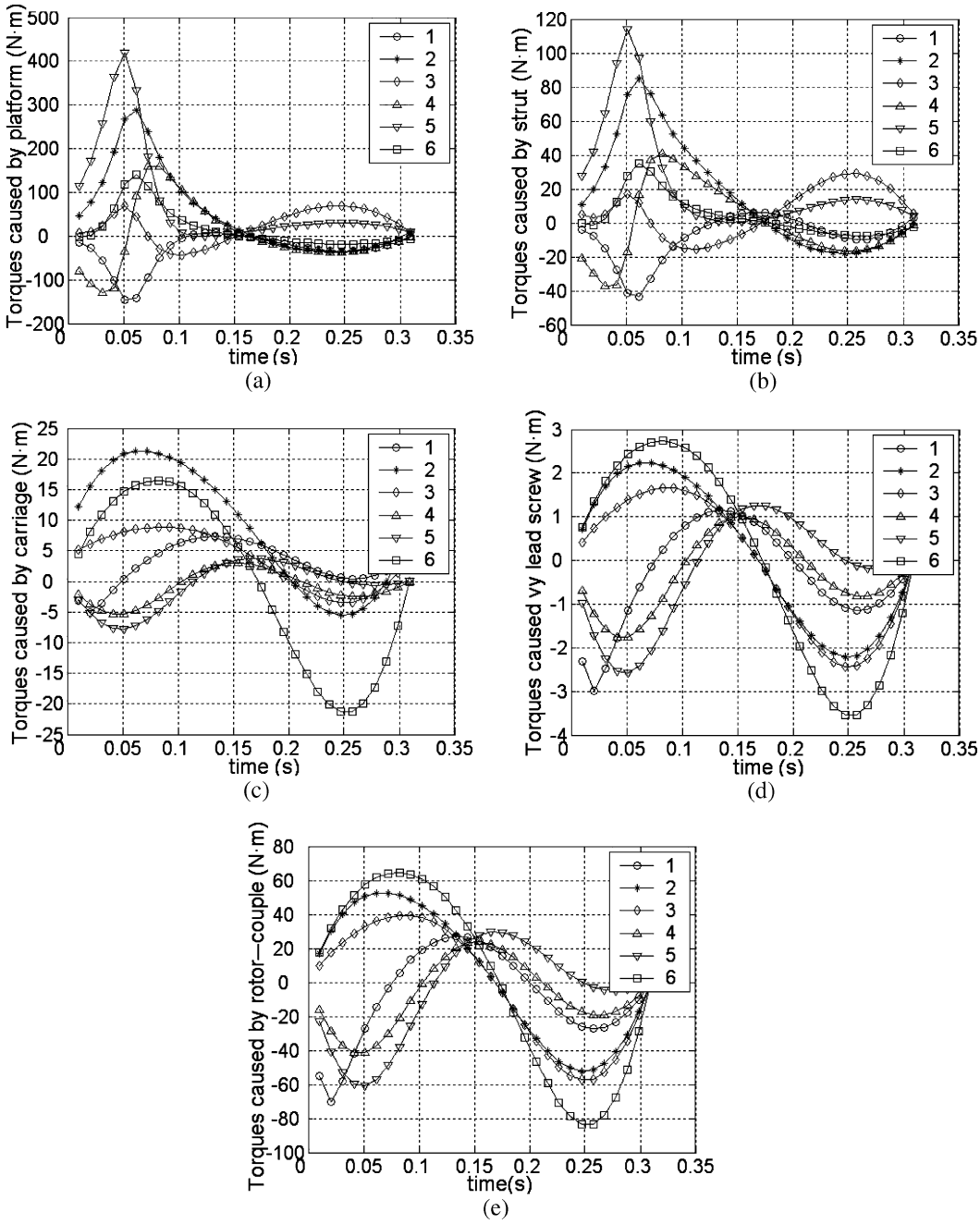

Fig. 6. Variations of torques caused by the moving platform (a), torques caused by the strut (b), torques caused by the carriage (c), torques caused by the lead screw (d), and torques caused by the motor rotor and couple (e) vs. time.

rotation inertia of motor–coupler–screw should be included for the exact dynamic model used for the design of the control law or the estimation of servomotor parameters for the parallel manipulators. The procedure described in this paper can be applied to other types of out-parallel manipulators.

Acknowledgments

This research has been jointly sponsored by the National Natural Science Foundation of China (Grant No. 60534020), the 973 National Key Basic Research Program of China (Grant No. 2006CB705400), and the China Postdoctoral Science Foundation (Grant No. 20070410719). We would also like to thank the anonymous reviewers for their very useful comments.

References

1. J. P. Merlet, *Parallel Robots*, 2nd ed. (Kluwer Academic, Dordrecht, 2005).
2. L. W. Tsai, *Robot Analysis—The Mechanics of Serial and Parallel Manipulators* (John Wiley and Sons, New York, 1999).
3. Z. Huang, Y. F. Fang and L. F. Kong, *Theory of Parallel Robotic Mechanisms and Control* (in Chinese) (China Machine Press, Beijing, 1997).
4. K. Harib and K. Srinivasan, "Kinematic and dynamic analysis of Stewart platform-based machine tool structures," *Robotica* **21**(5), 541–554 (2003).
5. S. Riebe and H. Ulbrich, "Modelling and online computation of the dynamics of a parallel kinematic with six degrees-of-freedom," *Arch. Appl. Mech.* **72**(11–12), 817–829 (2003).
6. J. C. M. Carvalho and M. Ceccarelli, "A closed-form formulation for the inverse dynamics of a Cassino parallel manipulator," *Multibody Syst. Dyn.* **5**(2), 185–210 (2001).

https://doi.org/10.1017/S0263574708004657 Published online by Cambridge University Press

7. B. Dasgupta and T. S. Mruthyunjaya, "Closed-form dynamic equations of the Stewart platform through the Newton–Euler approach," *Mech. Mach. Theory* **33**(7), 993–1012 (1998).
8. B. Dasgupta and T. S. Mruthyunjaya, "A Newton–Euler formulation for the inverse dynamics of the Stewart platform manipulator," *Mech. Mach. Theory* **33**(8), 1135–1152 (1998).
9. W. Khalil and S. Guegan, "A Novel Solution for the Dynamic Modeling of Gough–Stewart Manipulators," *Proceeding of the 2002 IEEE International Conference on Robotics and Automation*, Washington, USA (2002) pp. 817–822.
10. W. Q. D. Do and D. C. H. Yang, "Inverse dynamic analysis and simulation of a platform type of robot," *J. Rob. Syst.* **5**(52), 209–227 (1988).
11. Z. Ji, "Study of the Effect of Leg Inertia in Stewart Platform," *Proceeding of the 1993 IEEE International Conference on Robotics and Automation*, Atlanta, USA (1993) pp. 212–226.
12. W. Khalil and S. Guegan, "Inverse and direct dynamic modeling of Gough–Stewart robots," *IEEE Trans. Rob.* **20**(4), 755–761 (2004).
13. B. Dasgupta and P. Choudhury, "A general strategy based on the Newton–Euler approach for the dynamic formulation of parallel manipulators," *Mech. Mach. Theory* **34**(6), 801–824 (1999).
14. S. S. Lee and J. M. Lee, "Design of a general purpose 6-DOF haptic interface," *Mechatronics* **13**(7), 697–722 (2003).
15. K. M. Lee and D. K. Shan, "Dynamic analysis of a three-degrees-freedom in-parallel actuated manipulator," *IEEE Trans. Rob. Automat.* **4**(3), 361–367 (1988).
16. J. Lee, J. Albus, N. G. Dagalakis and T. Tsai, "Computer simulation of a parallel link manipulator," *Rob. Comput.-Integr. Manufact.* **5**(4), 333–342 (1989).
17. H. Pang and M. Shahinpoor, "Inverse dynamics of a parallel manipulator," *J. Rob. Syst.* **11**(8), 693–702 (1994).
18. Z. Geng, L. S. Haynes, T. D. Lee and R. L. Carroll, "On the dynamic and kinematic analysis of a class of Stewart platform," *Rob. Autonom. Syst.* **9**(4), 237–254 (1992).
19. G. Lebret, K. Liu and F. L. Lewis, "Dynamic analysis and control of a Stewart Platform manipulator," *J. Rob. Syst.* **10**(5), 629–655 (1993).
20. K. Miller and R. Clavel, "The Lagrange-based model of Delta-4 robot dynamics," *Robotersysteme* **8**(4), 49–54 (1992).
21. R. Ben-Horin, M. Shoham and S. Djerassi, "Kinematics, dynamics and construction of a planarly actuated parallel robot," *Rob. Comput.-Integr. Manufact.* **14**(2), 163–172 (1998).
22. M. J. Liu, C. X. Li and C. N. Li, "Dynamics analysis of the Gough–Stewart platform manipulator," *IEEE Trans. Rob. Automat.* **16**(1), 94–98 (2000).
23. M. Li, T. Huang, J. P. Mei, X. M. Zhao, D. G. Chetwynd and S. J. Hu, "Dynamic formulation and performance comparison of the 3-DOF modules of two reconfigurable PKMs-the TriVariant and the Tricept," *ASME J. Mech. Des.* **127**(6), 1129–1136 (2005).
24. A. Sokolov and P. Xirouchakis, "Dynamics analysis of a 3-DOF parallel manipulator with R-P-S joint structure," *Mech. Mach. Theory* **42**(5), 541–557 (2007).
25. F. Caccavale, B. Siciliano and L. Villani, "The Tricept robot: Dynamics and impedance control," *IEEE/ASME Trans. Mechatron.* **8**(2), 263–268 (2003).
26. J. Wang and C. M. Gosselin, "A new approach for the dynamic analysis of parallel manipulators," *Multibody Syst. Dyn.* **2**(3), 317–334 (1998).
27. S. Stefan, S. Laurian and R. Radu, "Inverse Dynamics of Star Parallel Manipulator," *Proceedings of the 2004 IEEE International Conference on Control Applications*, Taipei, Taiwan (2004) pp. 333–337.
28. L. W. Tsai, "Solving the inverse dynamics of a Stewart–Gough manipulator by the principle of virtual work," *ASME J. Mech. Des.* **122**(1), 3–9 (2000).
29. Z. Q. Zhu, J. S. Li, Z. X. Gan and H. Zhang, "Kinematic and dynamic modelling for real-time control of Tau parallel robot," *Mech. Mach. Theory* **40**(9), 1051–1067 (2005).
30. A. Codourey, "Dynamic modeling of parallel robots for computed-torque control implementation," *Int. J. Rob. Res.* **17**(2), 1325–1336 (1998).
31. A. Codourey and E. Burdet, "A Body Oriented Method for Finding a Linear Form of the Dynamic Equations of Fully Parallel Robot," *Proceeding of the 1997 IEEE International Conference on Robotics and Automation*, Albuquerque, USA (1997) pp. 1612–1618.
32. Y. J. Zhao, Z. Y. Yang and T. Huang, "Inverse dynamics of Delta robot based on the principle of virtual work," *Trans. Tianjin Univ.* **11**(4), 268–273 (2005).
33. S. Staicu and D. C. Carp-Ciocardia, "Dynamic Analysis of Clavel's Delta Parallel Robot," *Proceedings of the 2003 IEEE International Conference on Robotics and Automation*, Taipei, Taiwan (2003) pp. 4116–4121.
34. C. D. Zhang and S. M. Song, "An effective method for inverse dynamics manipulators based upon virtual work principle," *J. Rob. Syst.* **10**(5), 605–627 (1993).
35. J. Gallardo, J. M. Rico and A. Frisoli, "Dynamics of parallel manipulators by means of screw theory," *Mech. Mach. Theory* **38**(11), 1113–1131 (2003).
36. A. Muller and P. Maiber, "A Lie-group formulation of kinematics and dynamics of constrained MBS and its application to analytical mechanics," *Multibody Syst. Dyn.* **9**(4), 311–352 (2003).
37. W. A. Khan, V. A. Krovi, S. K. Saha and J. Angeles, "Recursive kinematics and inverse dynamics for a planar 3R parallel manipulator," *ASME J. Dyn. Syst., Meas. Control* **127**(4), 529–536 (2005).
38. A. B. Koteswara Rao, S. K. Saha and P. V. M. Rao, "Dynamics modelling of hexaslides using the decoupled natural orthogonal complement matrices," *Multibody Syst. Dyn.* **15**(2), 159–180 (2006).
39. F. F. Xi, O. Angelico and R. Sinatra, "Tripod dynamics and its inertia effect," *ASME J. Mech. Des.* **127**(1), 144–149 (2005).
40. M. K. Lee and K. W. Park, "Kinematics and dynamics analysis of a double parallel manipulator for enlarging workspace and avoiding singularities," *IEEE Trans. Rob. Automat.* **15**(6), 1024–1034 (1999).
41. K. Sugimoto, "Kinematics and dynamic analysis of parallel manipulator by means of motor algebra," *ASME J. Mech., Transm. Automat. Des.* **109**(1), 3–7 (1987).
42. T. Geike and J. McPhee, "Inverse dynamic analysis of parallel manipulators with full mobility," *Mech. Mach. Theory* **38**(6), 549–562 (2003).
43. J. McPhee, P. Shi and J. C. Piedboeuf, "Dynamics of multibody systems using virtual work and symbolic programming," *Math. Comput. Model. Dyn. Syst.* **8**(3), 137–155 (2002).
44. J. M. Selig and P. R. McAree, "Constrained robot dynamics II: Parallel machines," *J. Rob. Syst.* **16**(9), 487–498 (1999).
45. C. M. Gosselin, "Parallel computational algorithms for the kinematics and dynamics of planar and spatial parallel manipulators," *ASME J. Dyn. Syst., Meas. Control* **118**(1), 22–28 (1996).
46. G. J. Wiens, S. A. Shamblin and Y. H. Oh, "Characterization of PKM dynamics in terms of system identification," *Proc. Instn. Mech. Engrs. Part K: J. Multi-Body Dyn.* **216**(1), 59–72 (2002).
47. Y. K. Yiu, H. Cheng, Z. H. Xiong, G. F. Liu and Z. X. Li, "On the Dynamics of Parallel Manipulators," *Proceeding of the 2001 IEEE International Conference on Robotics and Automation*, Seoul, Korea (2001) pp. 3766–3771.
48. H. Cheng, Y. K. Yiu and Z. X. Li, "Dynamics and control of redundantly actuated parallel manipulators," *IEEE Trans. Mechatron.* **8**(4), 483–491 (2003).
49. Q. Huang, H. Hadeby and G. Sohlenius, "Connection method for dynamic modelling and simulation of parallel kinematic mechanism (PKM) machines," *Int. J. Adv. Manufact. Technol.* **19**(3), 163–173 (2002).
50. S. Kemal Ider, "Inverse dynamics of parallel manipulators in the presence of drive singularities," *Mech. Mach. Theory* **40**(1), 33–44 (2005).

https://doi.org/10.1017/S0263574708004657 Published online by Cambridge University Press